



Modeling of a Sequential Two-Stage Combustor

R.C. Hendricks, N.-S. Liu, and J.R. Gallagher
Glenn Research Center, Cleveland, Ohio

R.C. Ryder and A. Brankovic
Flow Parametrics, Bear, Delaware

J.A. Hendricks
Diligent Design, Toledo, Ohio

The NASA STI Program Office . . . in Profile

Since its founding, NASA has been dedicated to the advancement of aeronautics and space science. The NASA Scientific and Technical Information (STI) Program Office plays a key part in helping NASA maintain this important role.

The NASA STI Program Office is operated by Langley Research Center, the Lead Center for NASA's scientific and technical information. The NASA STI Program Office provides access to the NASA STI Database, the largest collection of aeronautical and space science STI in the world. The Program Office is also NASA's institutional mechanism for disseminating the results of its research and development activities. These results are published by NASA in the NASA STI Report Series, which includes the following report types:

- **TECHNICAL PUBLICATION.** Reports of completed research or a major significant phase of research that present the results of NASA programs and include extensive data or theoretical analysis. Includes compilations of significant scientific and technical data and information deemed to be of continuing reference value. NASA's counterpart of peer-reviewed formal professional papers but has less stringent limitations on manuscript length and extent of graphic presentations.
- **TECHNICAL MEMORANDUM.** Scientific and technical findings that are preliminary or of specialized interest, e.g., quick release reports, working papers, and bibliographies that contain minimal annotation. Does not contain extensive analysis.
- **CONTRACTOR REPORT.** Scientific and technical findings by NASA-sponsored contractors and grantees.

- **CONFERENCE PUBLICATION.** Collected papers from scientific and technical conferences, symposia, seminars, or other meetings sponsored or cosponsored by NASA.
- **SPECIAL PUBLICATION.** Scientific, technical, or historical information from NASA programs, projects, and missions, often concerned with subjects having substantial public interest.
- **TECHNICAL TRANSLATION.** English-language translations of foreign scientific and technical material pertinent to NASA's mission.

Specialized services that complement the STI Program Office's diverse offerings include creating custom thesauri, building customized databases, organizing and publishing research results . . . even providing videos.

For more information about the NASA STI Program Office, see the following:

- Access the NASA STI Program Home Page at <http://www.sti.nasa.gov>
- E-mail your question via the Internet to help@sti.nasa.gov
- Fax your question to the NASA Access Help Desk at 301-621-0134
- Telephone the NASA Access Help Desk at 301-621-0390
- Write to:
NASA Access Help Desk
NASA Center for AeroSpace Information
7121 Standard Drive
Hanover, MD 21076



Modeling of a Sequential Two-Stage Combustor

R.C. Hendricks, N.-S. Liu, and J.R. Gallagher
Glenn Research Center, Cleveland, Ohio

R.C. Ryder and A. Brankovic
Flow Parametrics, Bear, Delaware

J.A. Hendricks
Diligent Design, Toledo, Ohio

National Aeronautics and
Space Administration

Glenn Research Center

Acknowledgments

The authors wish to thank Dr. Marvin Goldstein, the NASA Glenn Research Center Strategic Research Fund, and the Revolutionary Aeropropulsion Concepts Project at NASA Glenn Research Center for support of this work and Timothy M. Roach for air-solid modeling assistance.

Trade names or manufacturers' names are used in this report for identification only. This usage does not constitute an official endorsement, either expressed or implied, by the National Aeronautics and Space Administration.

Available from

NASA Center for Aerospace Information
7121 Standard Drive
Hanover, MD 21076

National Technical Information Service
5285 Port Royal Road
Springfield, VA 22100

Available electronically at <http://gltrs.grc.nasa.gov>

MODELING OF A SEQUENTIAL TWO-STAGE COMBUSTOR

R.C. Hendricks, N.-S. Liu, and J.R. Gallagher
National Aeronautics and Space Administration
Glenn Research Center
Cleveland, Ohio 44135

R.C. Ryder and A. Brankovic
Flow Parametrics
Bear, Delaware 19701

J.A. Hendricks
Diligent Design
Toledo, Ohio 43614

ABSTRACT

A sequential two-stage, natural gas fueled power generation combustion system is modeled to examine the fundamental aerodynamic and combustion characteristics of the system. The modeling methodology includes CAD-based geometry definition, and combustion computational fluid dynamics analysis. Graphical analysis is used to examine the complex vortical patterns in each component, identifying sources of pressure loss. The simulations demonstrate the importance of including the rotating high-pressure turbine blades in the computation, as this results in direct computation of combustion within the first turbine stage, and accurate simulation of the flow in the second combustion stage. The direct computation of hot-streaks through the rotating high-pressure turbine stage leads to improved understanding of the aerodynamic relationships between the primary and secondary combustors and the turbomachinery.

INTRODUCTION

Two-stage or sequential combustors in power generation turbine engines are designed to utilize lean fuel-air mixtures to reduce pollutant emissions (NO_x , CO, UHC), and produce lower turbine inlet temperatures to enhance turbine durability. Theoretical analysis indicates that in the limit of many stages, achieving an isothermal turbine that performs close to the Carnot cycle thermal efficiency limit should be possible (Liu and Sirignano (2001)), yet this has been difficult to realize in practical, commercially viable machines (Ryder et al. (2003)). In this work we examine the aerodynamic, mixing, cooling and combustion characteristics of a two-stage combustion system including the rotating high-pressure turbine, using combustion computational fluid dynamics (CFD) simulations. The simulation is performed within a single computational domain, with full coupling between the two combustors and the rotating high-pressure (HP) turbine. Typically, combined combustor-turbomachinery computations are performed using code-coupling methods (Turner et al. (2002)) that patch boundary conditions at artificial interfaces embedded within the components. In the present calculation, one continuous flow path is modeled that includes both combustors and the rotating turbine stage.

The combustor/turbine geometry and operating conditions are similar to the high output ABB industrial gas turbine system and includes the primary burner and diffusion system, first turbine vane and blade, and secondary or reheat combustor and the associated diffusion system. Further discussion is provided in appendix A.

SEQUENTIAL COMBUSTOR OPERATION

The overall concept of the two-stage combustor, sometimes termed inter-turbine burner (ITB), is related in the isometric solid model of Figure 1. We have chosen to represent only the combustor region of the gas-turbine engine while the inlet, compressor, power turbine, nozzle, secondary flow paths and basic foundation are not shown.

In this system, compressor air is bifurcated at the last stage of compression with only the first stage combustor air being compressed to high pressure of about 30 atm. The remainder of the engine air, at about 15 atm, passes through the high-pressure turbine disk and fed into the second stage combustor. This air provides cooling for the high turbine disk and cavity. Other concepts using all the high pressure air are readily envisioned.

Sequential Combustor

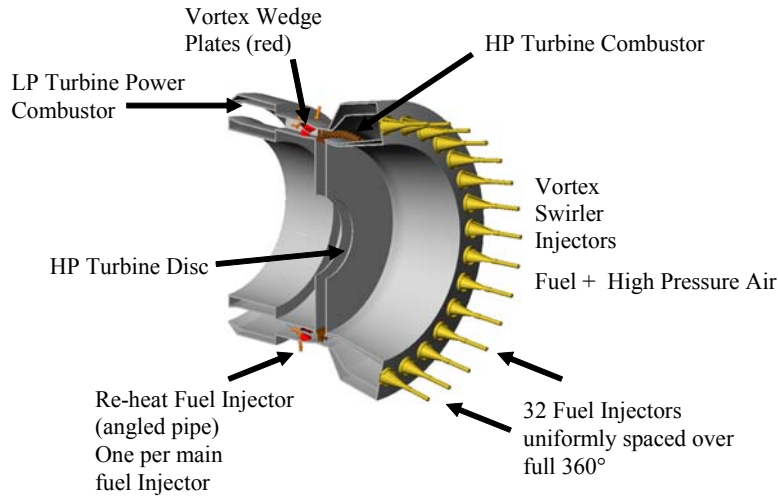


Figure 1. CAD solid model of two-stage axial flow combustor for power generation gas-turbine engine (similar to ABB engine configuration).

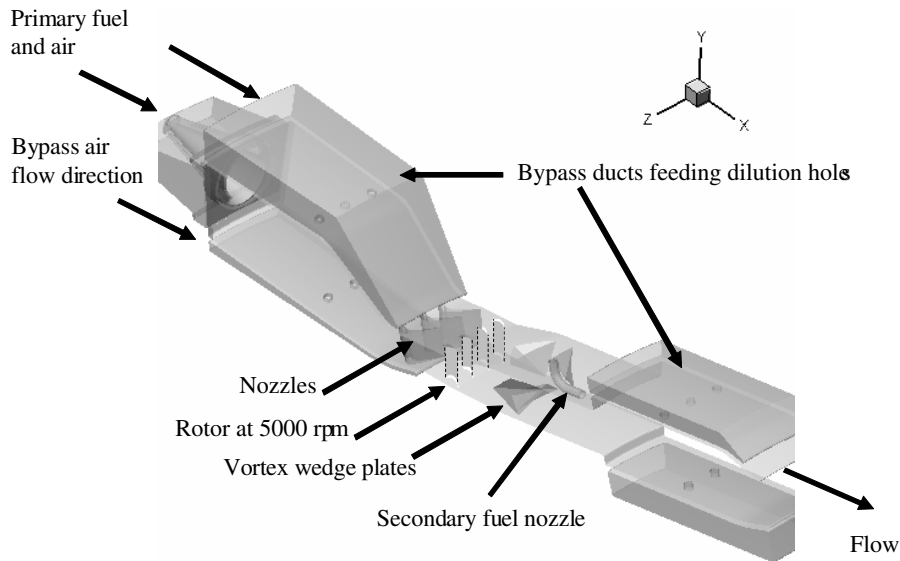


Figure 2. CAD solid model of typical section flow path showing the metal surfaces that define the gas flow path. Note, flow direction is reversed from that shown in Figure 1.

The high-pressure air is fed into a plenum with 32 vortex swirler (tangential entry) fuel injectors, arranged in a circular pattern. These injectors are designed to handle gaseous and liquid fuels through separate injectors, and must be capable of operating in dual-mode fueling for peak loads. In this work we concentrate on gaseous methane fuel injection as used under base load operating conditions. The specifics of the design are omitted, yet high-pressure combustion air is drawn into the swirler through opposing air streams forming a vortical flow that mixes with the fuel. This vortex is ejected into the combustor, much like a smoke ring, that reacts and burns in a lean mix

low Mach number (0.25) condition. The vortex pattern tends to stabilize the combustion process.

These gases are re-accelerated to the nozzles and fed through the high-turbine that powers the compressor and into a diffuser section upstream of the second stage combustor. In this section, a series of delta-wedges, with apexes set toward the fuel stems, swirls the flow field providing mixing of the turbine exhaust and turbine cooling air with the fuel. This lean mixture is swirled into the second stage combustor where it burns and exhausts to the power turbine. Our analysis does not include the LP or power turbine.

COMBUSTOR COMPUTATIONAL MODEL

A 1/32nd circular arc sector of the combustor flow path geometry is illustrated in Figure 2, with flow direction reversed from that shown in Figure 1. The model is a CAD solid model showing all significant metal surfaces in the flow path. The swirler outlet, the first stage combustor cavity, nozzles, high turbine blades, wedges, fuel injector and second stage combustor with feed air (diffusion air) hole simulation constitute the flow path. This is the geometry model for analysis herein. A complete description of the sequential combustion configuration is given in appendix C.

With the geometry defined, a solid model was formed and via Boolean subtraction the “air-solid” model was extracted and a coarse grid formed using an automated mesh generator consisting of approximately 1.5 million tetrahedral elements. Boundary conditions for the air and fuel flows were applied to the first and second stage combustors, with periodic side walls. The first stage HP turbine rotated at 5000 rpm, and was invoked in the model by applying a moving-wall boundary condition to the blade surface.

The inflow boundary conditions used in the simulation are as follows. Primary combustor inlet air flow entered at static pressure of 30 atm, static temperature of 800 °K, and at a mass flow rate of 20.65 kg/sec per sector (32 sectors total). The combustor operates in the lean stoichiometric regime, with the equivalence ratio of the primary combustor, not including any dilution air, is 0.604, with gaseous methane fuel introduced at 300 °K, and at a mass flow rate of 0.7365 kg/sec. Primary combustor plenum (or diffuser) air was introduced at 32 atm and at 800 °K, at a combined mass flow rate of 9.0 kg/sec for both inboard and outboard components of the diffuser. Plenum air was split in the ratio of 53 percent into the outboard duct, and 47 percent into the inboard duct.

Flow into the secondary combustor consists of the vitiated, hot products of combustion from the primary combustor, rotated through the HP turbine stage with associated decrease in enthalpy, and combined with fresh fuel injection and fresh bypass air entering in through the diffuser plenum. Secondary combustor fuel flow rate was 0.427 kg/sec, with a fuel temperature of 300 °K. The shroud flow for the secondary combustor was 7.85 kg/sec, split in the ratio 57 percent outer, 43 percent inner.

The operating parameters for the industrial gas turbine are generated in more detail in appendix B. These results provided the basis for calculations reported herein.

The FPVortexTM flow solver (Ryder and McDivitt (2000)) was used to compute the combustion flow field. The code solved the Reynolds-averaged Navier-Stokes (or RANS) equations, using the two-equation (or k-ε) turbulence

model for closure; wall functions were applied at all solid surfaces. Combustion was simulated using the eddy dissipation concept (EDC) heat release model (Magnussen and Hjertager (1977), Warnatz et al. (1996), and Peters (2000)). Standard turbulence and mixing parameters were used in the simulation. The computational model consisting of 1.5 million tetrahedral elements was stored in an unstructured database format. The code was run in parallel on networked workstations, with linear performance improvement as additional CPUs were added to the network. Validation cases for basic aerodynamic and combustion problems are discussed in Ebrahimi et al. (2001), while additional applications of the code to complex combustion problems are discussed in Hendricks et al. (2001).

COMPUTATIONAL RESULTS

Isotherms

The combined thermal-flow patterns are illustrated in Figure 3, with emphasis placed on extracting the high temperature flow features. The evidence of strong swirling is noted along with the distortions that are propagated downstream through the turbine and into the second stage combustor. The first stage combustor region is enlarged for enhanced viewing.

In Figure 4, emphasis is placed on extracting the lower temperature combustion features. Combustor hot spots are noted in elemental sections taken a discrete distance from upstream to downstream illustrating local heating that is obscured by and encased within the vortical flows.

Vortical Flow Pattern

The complexity of this flow field is further explored in Figure 5 that shows the hot products of combustion that originally form downstream of the main fuel injector. The combustor-turbine geometry is shown in the background. The combustion zone rotates with high vorticity, and enters the HP turbine stage. The swirled, vitiated flow then enters the second combustor, with additional fuel injection. The secondary fuel injection is axial, and forms a hot jet issuing into the secondary combustor. Velocity vectors illustrate the rotational aspects of the hot flow streak.

Hot Streak Simulation

Perhaps the most interesting feature of the computations is the interaction of the combustor flow and the high turbine stage. Figure 6 illustrates three separate stages of the thermal-flow fields (i) the swirler and first stage combustor (ii) the nozzles and turbine blades (iii) the second stage combustor. The radial slices were extracted at different radial distances from the engine centerline. From this perspective, one can readily see how distortions in the first stage combustor feed into the nozzles, are partially diffused and feed into the high turbine blades.

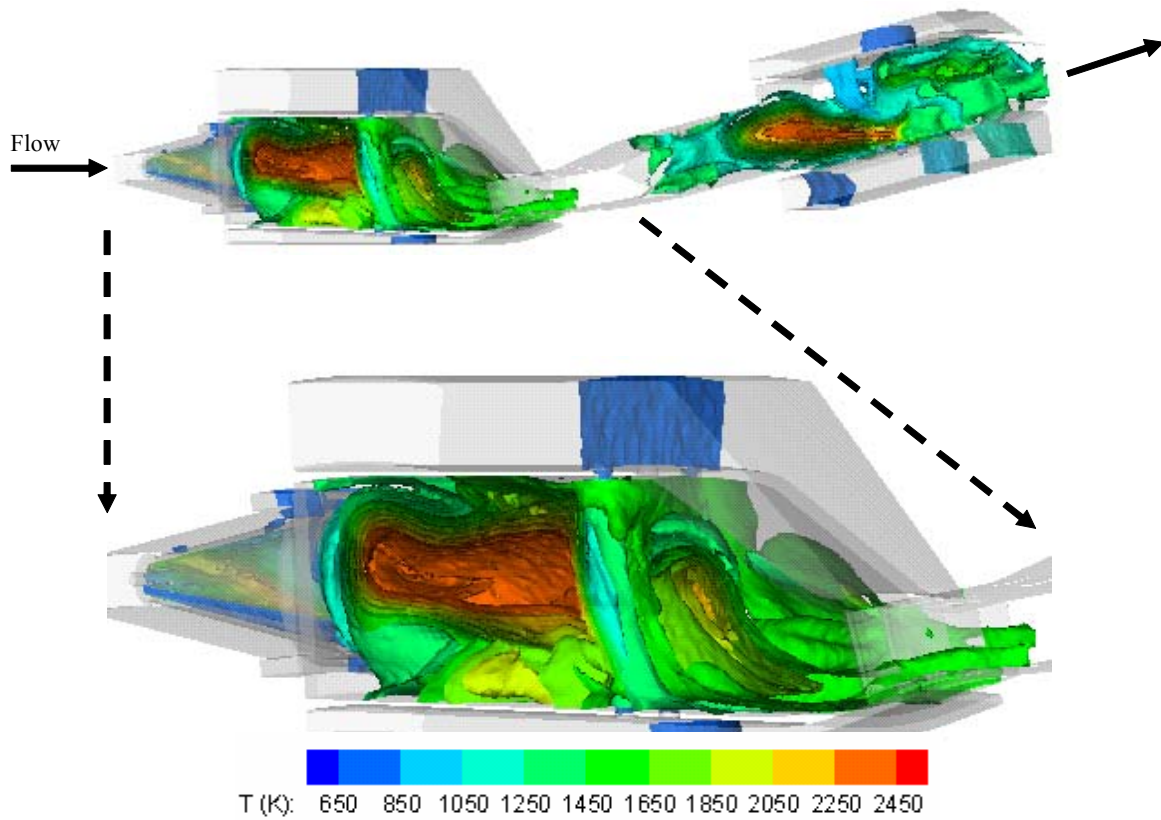


Figure 3. Computed isotherms in the two-stage combustor, with emphasis on the high temperature field. Hot products of combustion are generated downstream of the fuel injectors. Cool dilution air jets act to confine the combustion zones.

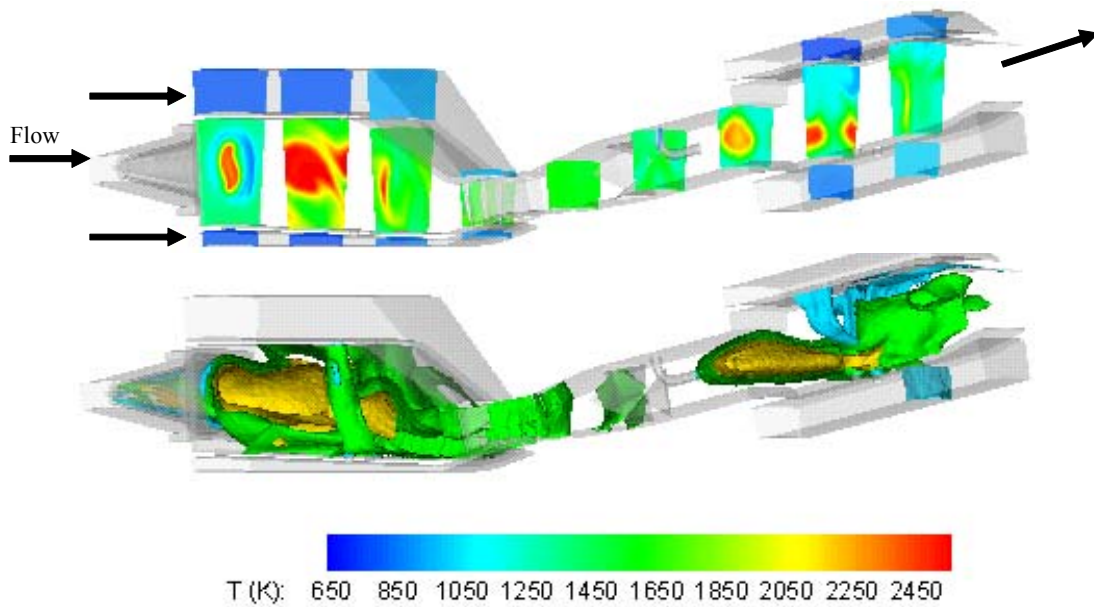


Figure 4. Axial slices showing computed temperature (upper), and 3D isotherms with emphasis on the low temperature field in the combustion zone (lower). The strong vortical combustion pattern is due to the swirling flow tangential entry combustion air that mixes with the fuel and stabilizes the flame inside the cone.

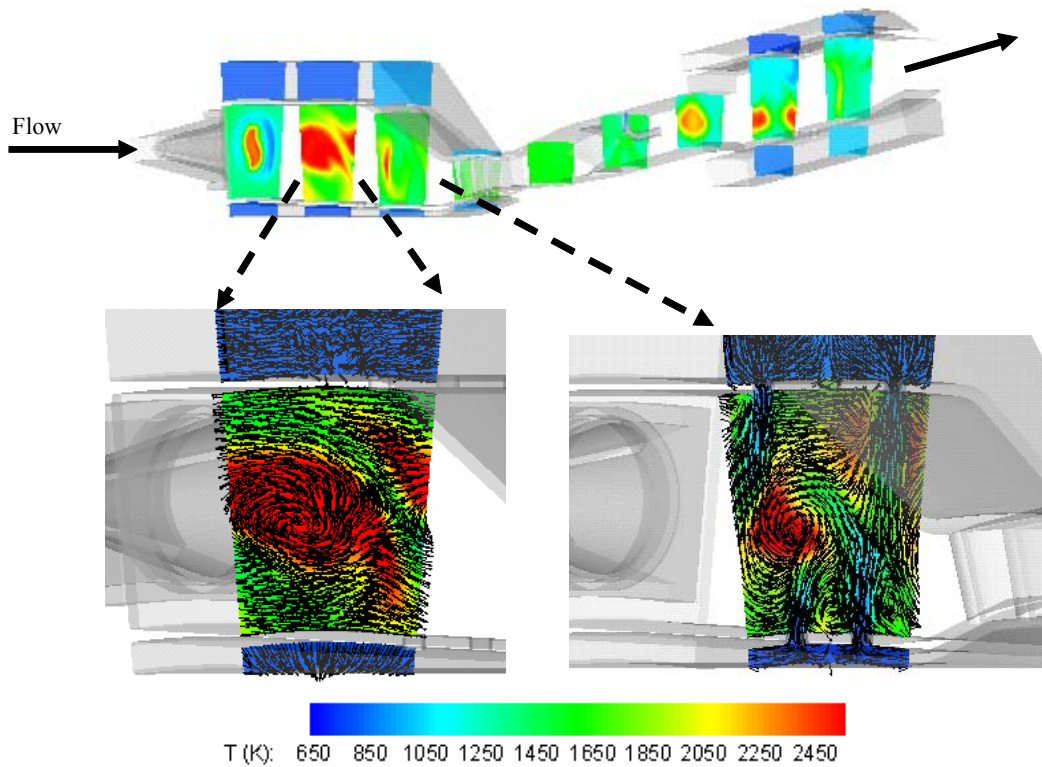


Figure 5. Details of computed temperature field in the primary (upstream) combustor. In the lower figures, cross-stream velocity vectors superposed on the temperature field show the main burning pattern.

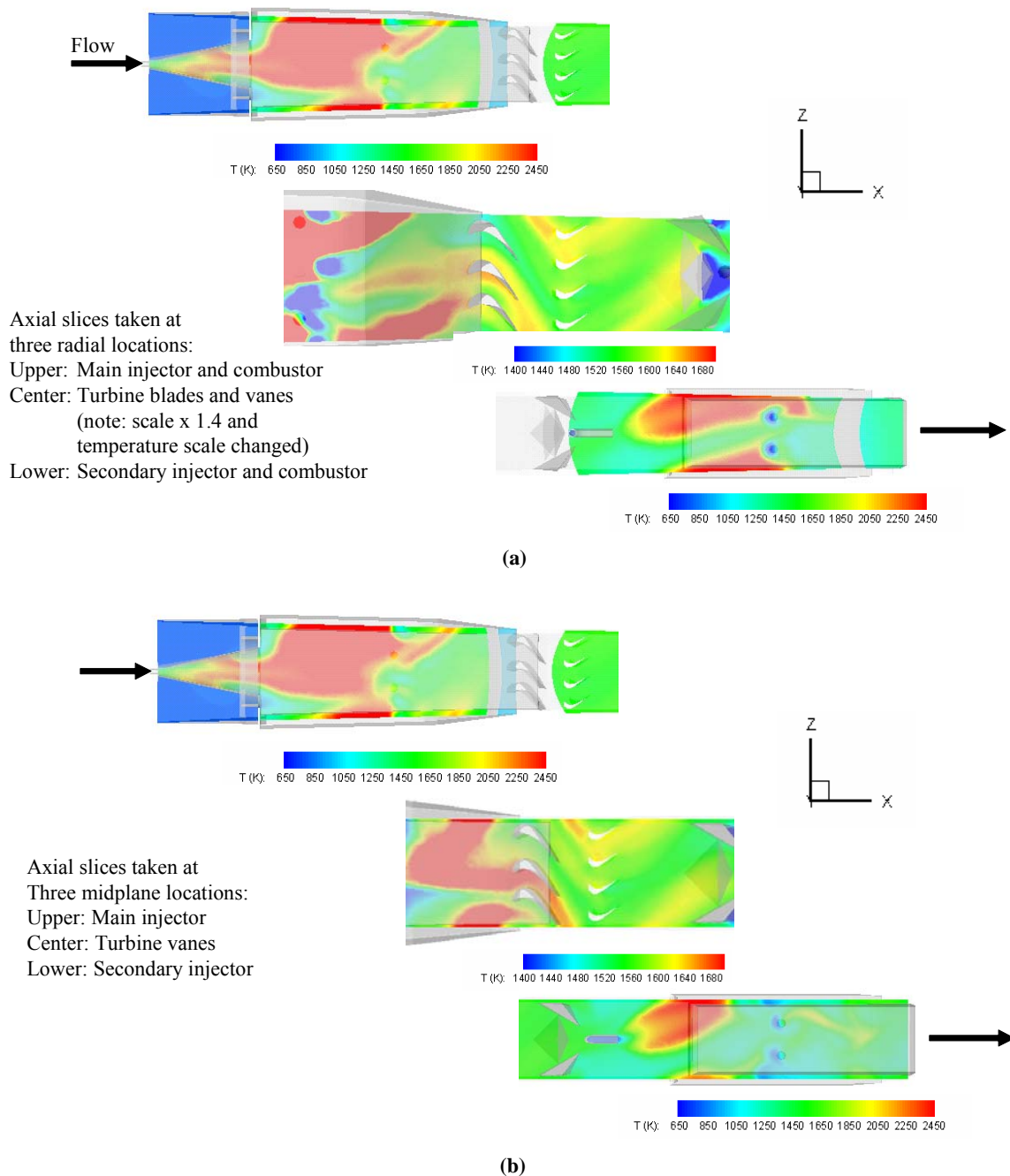


Figure 6. Non-uniformities in the thermal flow field for sequential two-stage combustor. Top: Primary injector/swirler and combustor. Center: Primary combustor nozzle-turbine blade interaction zone. Bottom: Second stage combustor. Note that temperature scales are adjusted among the frames, to highlight different flow patterns. Center figure shows direct computation of combustor hot streak entering HP turbine vane, rotating at 5000 rpm. The streak periodically re-enters the computation zone, and impinges the fuel nozzle in the secondary combustor. (a) Flow field slices taken at fixed planes relative to primary combustor (see fig. 7(a)). (b) Flow field slices taken at midplane of each sector (see fig. 7(b)).

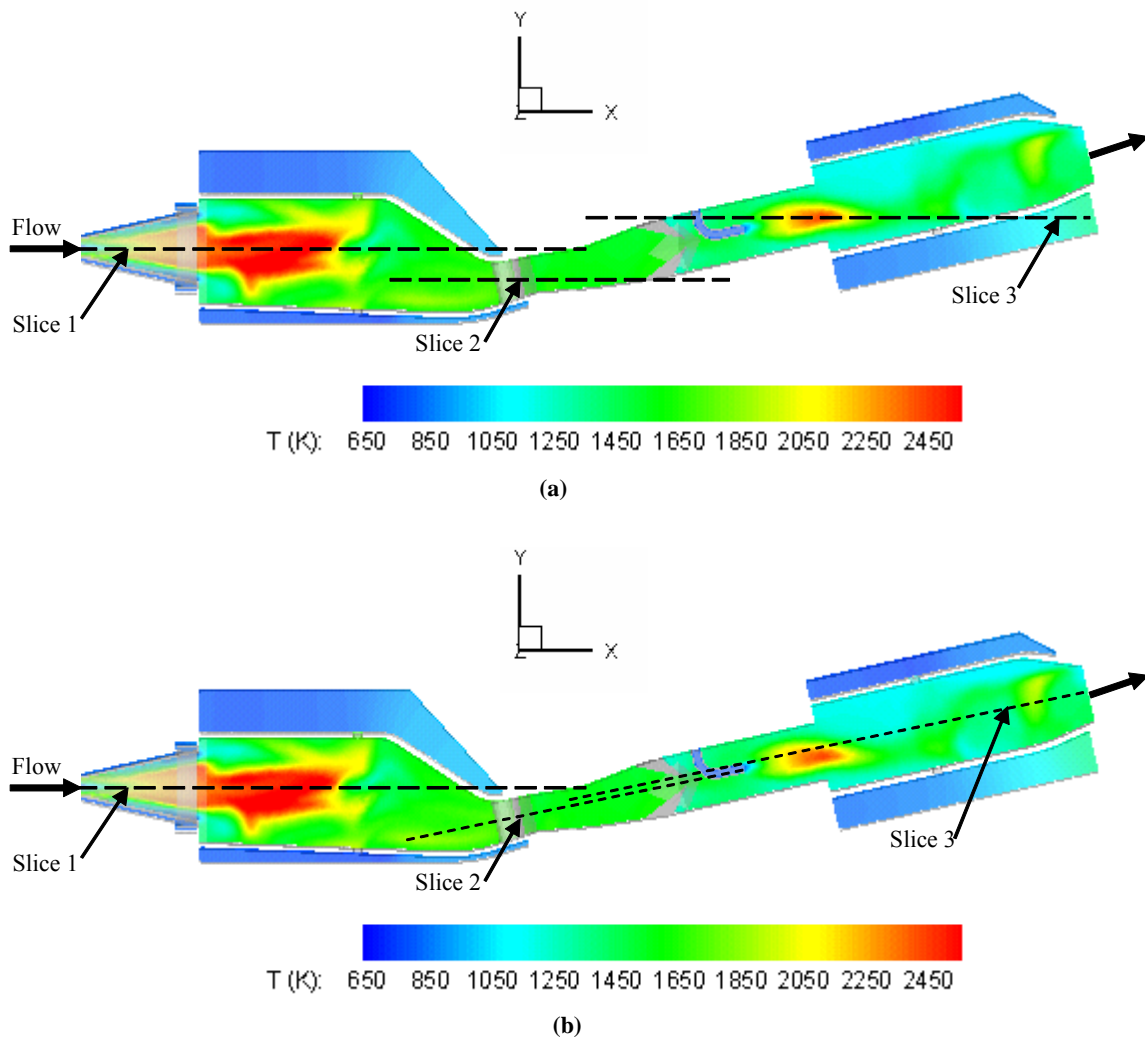


Figure 7. Computed static temperature field along the sequential combustion system. **(a)** Constant Y slice: (1) taken through center of primary combustor fuel nozzle, (2) taken at midpoint of turbine stage, (3) taken through center of secondary combustor fuel nozzle. Note: slice 2 is closest to the engine centerline, Slice 1 is further from the engine centerline, Slice 3 is furthest from the engine centerline (see fig 6(a)). **(b)** Midplane slice (1) taken through midplane of primary combustor, slice (2) taken through turbine stage, and slice (3) taken through the secondary combustor fuel nozzle (see fig. 6(b)).

The non-uniformity of the flow is readily observed as it enters the high turbine flow field as well as downstream as it enters the mixing and fueling zone of the second stage combustor. These non-uniformities are based on steady state flows, and therefore represent a snapshot in time of the actual flow field. In a full time-accurate simulation, the flow features and particularly the hot streak would most likely have enhanced differences with time resolved computations with coupled blade passing, cavity, seal (root and tip) and stator interactions. If one were to only picture the thermal-flow field along the central plane, as shown in Figure 7, it would not reveal the non-uniformities cited prior.

CONCLUSIONS

Sequential combustors are designed to provide a stable, lean burning, lower temperature alternative to single stage

combustors. The present combustion CFD analysis, featuring a coupled combustor-turbomachinery simulation, illustrates several of the key flow features associated with a particular implementation of a two-stage combustor. Lower power-turbine inlet (or primary combustor exit) temperature leads directly to improvements in blade life durability, efficiency and reduction in pollutant emissions.

Assessment of the thermal flow field from the compressor discharge to power turbine inlet requires careful monitoring. Computations herein illustrate the coupled nature of the field and distortions that alter both the flow to the high turbine and the low one as well. These non-uniformities impact engine efficiency.

APPENDIX A

Correct geometry and staging of compressors, combustors and turbines can simulate multi-spool operation on a single spool.

Consider the thermodynamic cycle of a conventional single-spool engine on a temperature-entropy diagram (Figure A-1).

Work necessary to drive the compressor W_c is exceeded by the turbine work W_t and the difference drives a generator. The amount of heat necessary to sustain this cycle Q , is given up by the addition of fuel w_f to a large amount of air w_a . Usually the fuel/air ratio is of the order of 0.02 to 0.03 kg-fuel/(kg-air). For flight gas turbine engines, thrust specific fuel consumption (TSFC), or SFC, is of the order 0.5 lbm-fuel/lbf-thrust-hour) (approx. 0.05 kg/N-hour).

Consider now the thermodynamic cycle of a staged-system (Figure A-2). This system has a low and high pressure compressor, combustor and turbine, yet all on a common spool. The compressor, combustor and turbine geometries as well as internal flows differ from the conventional single-spool engine.

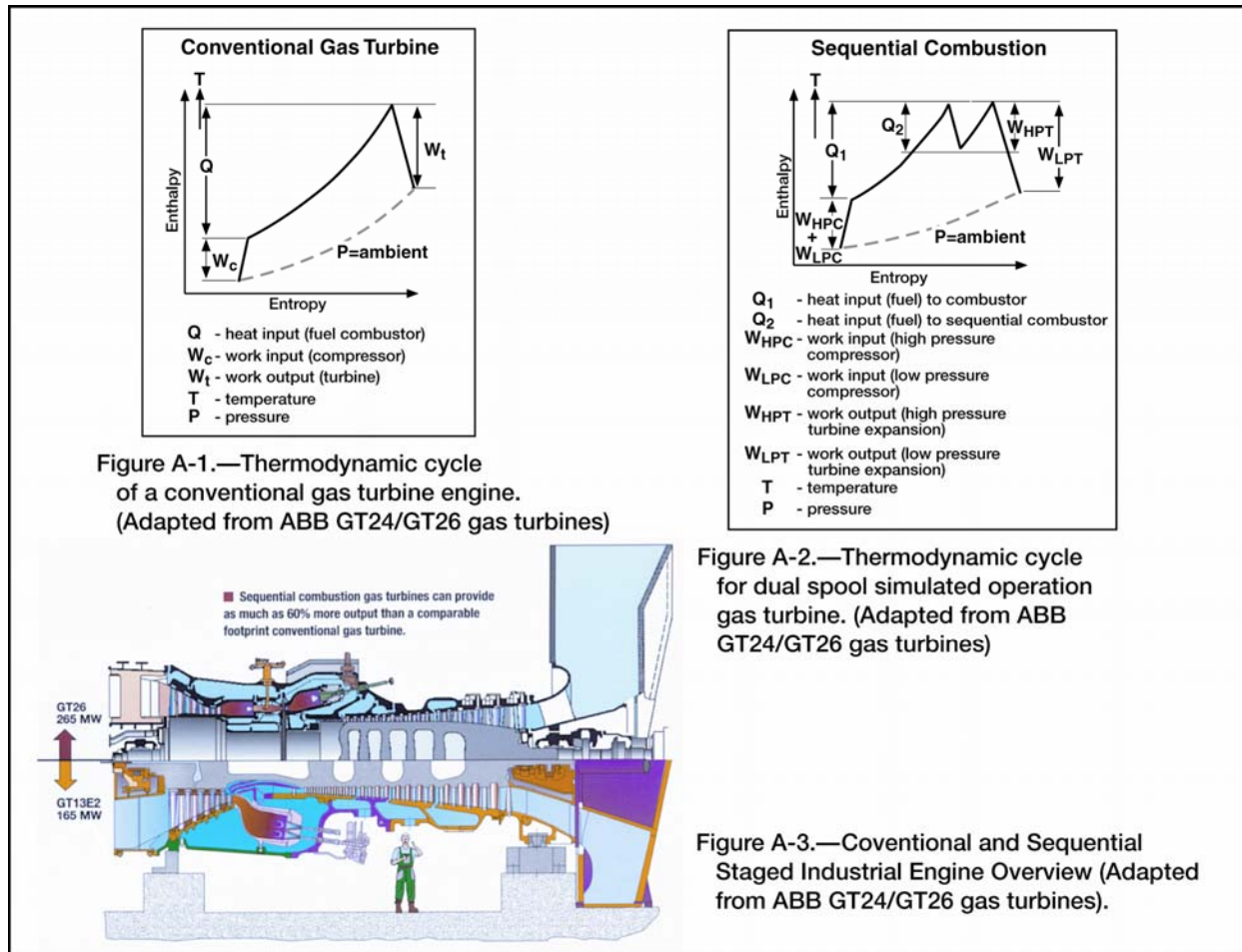
First the low-pressure or power-spool

Staged, low pressure compressor (LPC) air by-passes the high-pressure compressor (HPC), passing through the core wheel space of the high pressure turbine (HPT) into the low pressure staged-combustor (LPSC) where air is mixed with fuel (Q_2) and upstream combustion products to drive the low pressure turbine (LPT).

Second the high-pressure or the gas-generator spool

The non-staged air passes though yet another stage (or more) of compression (HPC) and fed into the high-pressure staged combustor (HPSC) where fuel is added as heat Q_1 . The fuel lean combustion products drive the HPT whose geometry has been altered to maintain high efficiency. The effluent is in turn passed to a pre-burner mixer where additional fuel as heat Q_2 is added to the staged low pressure air from the LPC. These products of combustion drive the LPT and power the generator.

The sequential two-staged combustor provides (a) high pressure low emissions gas to drive the HPC and (b) mixed products gas to drive the LPT providing two-spool equivalent operation on a single spool machine. Figure A-3 provides an overview of the conventional and sequential staged engines.



APPENDIX B—AN ESTIMATION OF ABB SEQUENTIAL COMBUSTOR OPERATING PARAMETERS

The sequential combustor modeled herein is based on information literature distributed by ABB Power Generation GT24/GT26 gas turbine technology division.

For the model here, we assumed the component and input parameters cited in tables 1 and 2. The initial set in table 1 and the modified and developed set in table 2. It is necessary to make several assumptions as to scale, temperature, pressure and on the flow splits as key information is lacking in the open literature and only the flow necessary to drive the gas generator part of the cycle is compressed to 30:1. The remaining inlet air is bypassed through the turbine disc for cooling and reducing the work load on the compressor. The overall pressure ratio and standard day inlet conditions are,

Compressor Pressure Ratio 30:1

Assume Standard Inlet Conditions 0.101325 MPa; 288.2 K; $\gamma = 1.4$

Compressor

High Pressure Burner

$$T_2 = T_1[\pi_c]^{(\gamma-1)/\gamma} = 288.2 (30)^{0.286/0.85} = 900 \text{ K}$$

Low Pressure Burner

$$T_2' = T_1[\pi_c]^{(\gamma-1)/\gamma} = 288.2 (15)^{0.286/0.85} = 735 \text{ K}$$

EV-High Pressure Burner

$$T_4 = 1523 \text{ K}$$

HP Turbine

$$\gamma = 1.33; \pi_{hp} = 0.48$$

$$T_5 = T_4 \{1 - [1 - \pi_{hp}^{(\gamma-1)/\gamma}] \eta_t\} = 1523 \{1 - [1 - (0.48)^{0.248}] 0.91\} = 1292 \text{ K}$$

Let $T_5 = 1300 \text{ K}$ (about 1000 °C given by ABB)

LP Turbine

Assert that reheat to $T_4 = 1523 \text{ K}$; $P_6 = 0.101325 \text{ MPa}$; $\gamma = 1.33$; $\eta_t = 0.90$

$$T_5 = T_4 \{1 - [1 - \pi_{hp}^{(\gamma-1)/\gamma}] \eta_t\} = 1523 \{1 - [1 - (1/15)^{0.248}] 0.90\} = 823 \text{ K}$$

Exhaust

$$T_{\text{exhaust-data}} = 833 \text{ K} \sim T_5$$

Mass Flow Rates

$$\dot{m}_{\text{available}} = \dot{m}_{\text{total}} \times 0.85$$

15% total air is component cooling air; part is high pressure (hp) (55% split or 8.2% of air) and part lp (45% split or 6.8% of air); some of this heated air is recovered other is parasitic and lost energy; air split is based on fueling split of 55% (EV burner) to 45% (low pressure burner)

Method 1: Fuel Flow Estimate

Btu/kWh = 9000 \rightarrow 2.5 = (Btu/s)/kW (conversion factor)

$$\begin{aligned} \text{Fuel Required} &= 166 \times 10^3 \text{ kW} \times 2.5 = 415 \times 10^3 \text{ Btu/s} \\ &= 1055 \text{ j/Btu} \times 415 \times 10^3 = 438 \text{ MJ/s} \end{aligned}$$

$50.2 \times 10^3 \text{ j/g}$ = Heat of Combustion

$$\text{Fuel required} = 0.438 \times 10^9 / 50.2 \times 10^3 = \dot{m}_f = \mathbf{8.721 \text{ kg/s}}$$

Method 2: Fuel Flow Estimate

166MW/37.9% efficient = 438 MW

$$\text{Fuel required} = 438 \times 10^3 \text{ j/s} / 50.2 \times 10^3 \text{ j/g} = 8.725 \text{ kg/s}$$

Method 3: Air Flow Estimate

Rob Ryder (Flow Parametrics) gives:

$$25 \text{ MW machine; } \dot{m}_t = 66.8 \text{ kg/s; } \dot{m}_f = 1.4 \text{ kg/s; } \phi = 0.55$$

And if one assumes $\eta = 34\%$ (elderly machine)

Required Equivalent Power = 25/0.34 = 73 MW

$$\dot{m}_f = 73 \times 10^3 / 50.2 = 1.45 \text{ kg/s}$$

$$f/a = \dot{m}_f / \dot{m}_{\text{air}} = 1.45 / 65.35 = 0.022$$

At 1.4 kg/s and $\phi_b = 0.55 \rightarrow \dot{m}_{\text{air}}]_{\text{burner}} = 1.4 / [0.55 \times 0.058] = 43.9 \text{ kg/s}$

Cooling Air = 22.9 kg/s

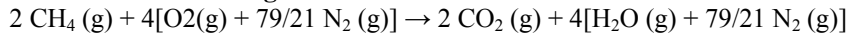
= 34.3% of total air flow

$$\dot{m}_f / \dot{m}_{\text{air}}]_{\text{burner}} = 0.0319$$

$$0.2 < (f/a) < 0.033$$

For the ABB-system, assume $(f/a) = \dot{m}_f / \dot{m}_{\text{air}} = \mathbf{0.022}$, $\rightarrow \dot{m}_{\text{air}} = 8.72 / 0.022 = \mathbf{396 \text{ kg/s}}$

Stoichiometric Burning



$$2 \times 16 \text{ gm} + 4 [32 + 105] \text{ gm}$$

$$\rightarrow \dot{m}_f / \dot{m}_{\text{air}} = 32 / (4 \times 137) = 0.058 \rightarrow \phi = 1.0$$

$$\dot{m}_{\text{air}} [1 + \dot{m}_f / \dot{m}_{\text{air}}] = 396 \text{ kg/s} [1 + \dot{m}_f / \dot{m}_{\text{air}}]$$

$$\dot{m}_{\text{air}} = 396 / [1 + 0.058] = 374.3 \text{ kg/s}$$

$$\dot{m}_f = 21.7 \text{ kg/s} \rightarrow \phi = 1.0$$

Burner Equivalence

$$\phi_b = \{ \dot{m}_f / [\dot{m}_{\text{total}} \times 0.85] \} / 0.058 = \{ 8.72 / [396 \times 0.85] \} / 0.058 = 0.47$$

(a little smaller than for the 25 MW machine where $\phi_b = 0.55$)

Total Work: Efficiency

$$\text{Work}_{t,e} = W_c + W_e = \dot{m}_{\text{air}} c_p \Delta T + W_e$$

$$= \{ \dot{m}_{\text{air}} \times 1 \times [0.55 (900 - 288) + 0.45 (735 - 288)] \} 10^{-3} + 166 \text{ MJ/s}$$

$$= 396 [0.55 \times (900 - 288) \times 1 + 0.45 \times (735 - 288) \times 1] / 1000 + 166 \text{ MJ/s}$$

$$= 379 \text{ MJ/s}$$

Efficiency = 166/379 = 43.8% (ABB gives 37.9%) \rightarrow 5.9% installation and engine external losses

While 43.8% is too high, it is within the uncertainty of the assumptions made herein; the parameters of Table 1 will serve as the basis for our CFD analysis.

Table 1. Component Modeling Modified Parameter Set.

[η = efficiency; \dot{m} = mass flow; $\phi = (f/a)/(f/a)_{\text{stoic}}$; f/a = fuel/air ratio;

dp/p = burner pressure drop; P_{ratio} = pressure ratio; T = temperature]

Component	Input Parameters
Compressor	$P_{\text{ratio}} = 30$; $\eta = 0.85$; $T_1 = 288 \text{ K}$; $T_2 = 900 \text{ K}$; $T'_2 = 735 \text{ K}$ 15% $\dot{m}_{\text{air-total}}$ = component cooling air split at 8.2% high pressure; 6.8% low pressure
Burner (EV)	$dp/p = 0.055$; $\eta = 0.987$; $\phi = 0.47$; 0.55 \dot{m}_f added
Turbine (High Pressure)	$\eta = 0.91$; $P_{\text{ratio}} = 0.48$; $T'_4 = 1523 \text{ K}$; $T'_5 = 1300 \text{ K}$
Burner (Turbine)	$dp/p = 0.025$; $\eta = 0.98$; $T_4 = 1523 \text{ K}$; 0.45 \dot{m}_f added
Turbine (Low Pressure)	$\eta = 0.91$; $P_{\text{ratio}} = 0.067$; $T_4 = 1523 \text{ K}$; $T_5 = 845 \text{ K}$
Exhaust	$T_{\text{exhaust}} = 833 \text{ K}$
$\dot{m}_{\text{air-total}}$: \dot{m}_f : \dot{m}_{cooling}	396 kg/s : 8.72 kg/s : 59.4 kg/s

Mean-Radius Stage Calculation—Isentropic Flow: Based on the method presented on p. 687, Elements of Gas Turbine Propulsion (Jack D. Mattingly, McGraw-Hill (1996))

For this simplified model, a combustor temperature of 1523 K, an engine speed of 3600 rpm and turbine radius of 1.25m is assumed. The initial temperature, based on the combustion studies can be higher than that given in the table, e.g., 1650K, yet will not impact P3 in a significant way. A further assumption that the flow is choked at the nozzle does have more of an impact on P3, yet can lead to unreasonable flow angle changes.

Natural gas is similar to methane with similar properties and to a first order represented as follows:
 $2 \text{CH}_4 (\text{g}) + 4[\text{O}_2(\text{g}) + 79/21 \text{N}_2 (\text{g})] \rightarrow 2 \text{CO}_2 (\text{g}) + 4[\text{H}_2\text{O} (\text{g}) + 79/21 \text{N}_2 (\text{g})]$

$$\text{Mol} = M_{\text{CO}_2} \times \text{CO}_2 + M_{\text{H}_2\text{O}} \times \text{H}_2\text{O} + M_{\text{N}_2} \times \text{N}_2 = 44 (2/21) + 18 (4/21) + 28 (15/21) = 27.6$$

Estimate

$$c_p = (\gamma / (\gamma - 1) R) = (1.3 / .3) 0.29 \text{ j/g-K} = 1260 \text{ m}^2/\text{s}^2 \quad (\text{j/kg} = \text{m}^2/\text{s}^2)$$

$$c = \sqrt{(\gamma R < T >)} = \sqrt{\{1.3 \times 290 \times [(1523 + 1300) / 2]\}} = 729 \text{ m/s}$$

$$\Delta h_o = c_p (T_{o1} - T_{o2}) = 1.26 (1523 - 1300) = 281 \text{ J/g} = 281 \text{E}3 \text{ J/kg} = 281 \text{E}3 \text{ m}^2/\text{s}^2$$

$$T_{t2} = T_{t1} = 1523 \text{ K}$$

$$T_2 = T_{t2} / [1 + ((\gamma - 1) / 2) M_2^2] = 1523 / (1 + 0.15 \times 1.07^2) = 1300 \text{ K}$$

[Note: $M_2 \sim 1$ is a reasonable starting point, $0.9 < M_2 < 1.15$]

$$V_2 = \sqrt{[2 c_p (T_{t2} - T_2)]} = \sqrt{[2 \times 1260 \times (1523 - 1300)]} = 750 \text{ m/s}$$

$$u_2 = V_2 \cos \alpha_2 = 750 \cos 67^\circ = 293 \text{ m/s}$$

$$v_2 = V_2 \sin \alpha_2 = 750 \sin 67^\circ = 690 \text{ m/s}$$

$$v_{2r} = v_2 - [r\omega = 1.25\text{m} \times 3600 \times 2\pi / 60 \text{ /s}] = 690 - 1.25 \times 377 = 690 - 471 = 220 \text{ m/s}$$

$$V_{2r} = \sqrt{[u_2^2 + v_{2r}^2]} = \sqrt{[293^2 + 220^2]} = 366 \text{ m/s}$$

$$\beta = \arctan [v_{2r} / u_2] = \arctan [220 / 293] = 36.9^\circ$$

$$M_{2r} = M_2 V_{2r} / V_2 = 1.07 (366 / 750) = 0.52$$

$$T_{t2r} = T_2 + V_{2r}^2 / (2c_p) = 1300 + 366^2 / (2 \times 1260) = 1353 \text{ K}$$

$$v_3 = 0$$

$$V_3 = u_3 = u_2 = 293 \text{ m/s}$$

$$v_{3r} = v_3 + [r\omega = 1.25\text{m} \times 3600 \times 2\pi / 60 \text{ /s}] = 0 + 471 = 471 \text{ m/s}$$

$$V_{3r} = \sqrt{[u_3^2 + v_{3r}^2]} = \sqrt{[293^2 + 471^2]} = 555 \text{ m/s}$$

$$\beta = \arctan [v_{3r} / u_3] = \arctan [471 / 293] = 58^\circ$$

$$T_{t3} = T_{t2} - r\omega(v_2 + v_3) / c_p = 1523 - 471 (690 + 0) / 1260 = 1265 \text{ K}$$

$$T_3 = T_{t3} - V_{3r}^2 / (2c_p) = 1265 - 555^2 / (2 \times 1260) = 1231 \text{ K}$$

$$M_3 = \sqrt{[(2 / (\gamma - 1)) ((T_{t3} / T_3) - 1)]} = \sqrt{[(2 / 0.3) ((1265 / 1231) - 1)]} = 0.43$$

$$M_{3r} = M_3 V_{3r} / V_3 = 0.43 (555 / 293) = 0.81$$

$$T_{t3r} = T_{t2r} = 1352 \text{ K}$$

$$P_{t2} = P_{t1} = 30 \text{ atm}$$

$$P_2 = P_{t2} (T_2 / T_{t2})^{[\gamma / (\gamma - 1)]} = 30 (1300 / 1523)^{[1.3 / .3 = 4.3333]} = 15.1 \text{ atm}$$

$$P_{t2r} = P_2 (T_{t2r} / T_2)^{[\gamma / (\gamma - 1)]} = 15.1 (1353 / 1300)^{[1.3 / .3 = 4.3333]} = 18 \text{ atm}$$

$$P_{t3r} = P_{t2r} = 19.2 \text{ atm}$$

$$P_{t3} = P_{t2} (T_{t3} / T_{t2})^{[\gamma / (\gamma - 1)]} = 30 (1265 / 1523)^{[1.3 / .3 = 4.3333]} = 13.4 \text{ atm}$$

$$P_3 = P_{t3} (T_3 / T_{t3})^{[\gamma / (\gamma - 1)]} = 13.5 (1231 / 1265)^{[1.3 / .3 = 4.3333]} = 12 \text{ atm}$$

ABB gives $P_3 \approx 15 \text{ atm}$ and $T_3 \approx 1300 \text{ K}$ so we start over. For example, if $M_2 = 0.9$ and machine speed set for 50 Hz vs 60 Hz, then following the same procedures, $P_3 = 15.8 \text{ atm}$; a 10% decrease in $(r\omega)$ which results in nearly a 10% increase in P_3 or 13.2 atm.; further if just the speed (50/60Hz) was considered in terms of $(r\omega)$, P_3 would increase to 13.8 atm. As we do not know the actual conditions, we will assume the above procedure reasonable for modeling purposes. Changing parameters to higher speed (5000 rpm) at blade radius of 1.2 m and inlet temperature of 1650 K gives $P_3 \sim 10 \text{ atm}$. For details see CFD analysis and Computational Results.

APPENDIX C—SEQUENTIAL COMBUSTOR ENGINE MODEL

Files for the Wedge Assembly Air Solid Model, as scaled from the ABB GT24/GT26 and associated ABB gas turbine literature, are provided on a CD-ROM as a supplement to this report. See the following section for specifics on these files or the CD_Contents.pdf on the CD.

Scaling: The following scaling factors were applied to the ABB pictorial representations in the open literature of the GT24/GT26 gas turbine. These values provide input to the CAD modeling program from which the base geometry was developed and through Boolean subtraction, the air solid model was formed for the sequential combustor thermophysical analysis.

2.637 ft/cm axial
1.846 ft/cm vertical
1.57 ft/cm horizontal

Scales: enlarged 5.5 cm = 6 ft
Scales: schematic 2.9 cm = 2.8 ft

Component Model Scales

Low pressure turbine last stage rotor

11.8 ft diameter (3600 mm)

High pressure turbine

8.9 ft diameter (2700 mm)

11th stage of compressor

7.2 ft diameter (2200 mm)

9.9 ft axial position (from front) (3025 mm)

EV-high pressure combustor

Angle 17 degrees off C.L. (centerline)

11.9 ft diameter (3620 mm)

2.8 ft length (850 mm)

1.7 ft height (500 mm)

1.8 ft to combustor neck (550 mm)

0.14 ft straight to inlet guide vanes (44 mm)

0.3 ft wide at turbine inlet (90 mm)

0.58 ft nozzle + turbine + transition to uniform passage (?) (180 mm)

Transition passage with wedges

2.4 ft length (75 mm) from turbine C.L. (centerline)

0.48 ft height (145 mm)

0.57 ft width-circumferential (175mm)

SEV-low pressure combustor

2.5 ft length (760 mm)

0.96 ft height (290 mm)

1.18 ft width-circumferential (360 mm)

6.75 ft ID (205 mm)

24 – per combustor stages per engine

EV-high pressure Swirler – 30 per engine combustor

Exit diameter: 0.48 ft (145 mm)

Swirler step: 0.057 ft (17 mm)

Length of swirler: 0.59 ft (18 mm)

Throat length: 0.16 ft (49 mm)

Throat diameter: 0.095 ft (29 mm)

Flow wedges

Open space between apexes = 1/2 passage (radial height)
0.8 passage (circumferential width)

WEDGE ASSEMBLY AIR SOLID MODEL

Timothy M. Roach

E-mail: Timothy.M.Roach@nasa.gov

Included are three folders, one for the original wedge assembly, one for the air solid of the wedge assembly, and one for the slice of the air solid. Within each folder there are 11 files including the native Unigraphics file (.prt), two Parasolid files (.x_t and .xmt_txt), an IGES file (.igs), two STEP files (203.stp and 214.stp), a VRML (.wrl) file and various JPEGs (.jpg) files.

Both the air solid model and the slice of the air solid model were last saved in version 17 of Unigraphics which means any version above and including 17 are able to open the files. The original wedge assembly model was last saved in Unigraphics NX2 (which would be Unigraphics version 20 if they kept the same naming convention) which means any version above and including NX2 are able to open the files.

Parasolid is the modeling kernel of Unigraphics and a few other solid modeling packages such as Solid Edge and would be the cleanest file to import into a CAD or Analysis package. Both types of Parasolid files are included.

Almost any CAD or Analysis package is able to import an IGES or a STEP file as those are common files. Out of the two formats, STEP would be the better choice. Included are two available options in Unigraphics to export both a STEP 203 and a STEP 214. Here at Glenn we use STEP 203. STEP 214 is possibly more common in the auto industry.

A VRML file is a virtual reality modeling language format. One can download a plugin for almost any standard web browser and view the VRML file. This is nice for people who do not have access to either a CAD or Analysis package. The plugin can be downloaded from <http://www.parallelgraphics.com/products/cortona/download/iexplore/>. To see the whole model click on the fit button in the bottom right-hand corner.

The JPEGs are an ISO view of each plus section views (both full and partial zoomed sections) of each model that shows what the models look like and show a little detail also.

REFERENCES

- Ebrahimi, H.B., Ryder, R.C., Brankovic, A., and Liu, N.-S., (2001) "A Measurement Archive for Validation of the National Combustion Code," AIAA-2001-0811.
- Hendricks, R.C., Shouse, D.T., Roquemore, W.M., Burrus, D.L., Duncan, B.S., Ryder, R.C., Brankovic, A., Gallagher, J.R., and Hendricks, J.A., (2001) "Experimental and Computational Study of Trapped Vortex Combustor Sector Rig with High-Speed Diffuser Flow," *Int. Journal of Rotating Machinery*, **7**(6), pp. 375-385.
- Liu, F. and Sirignano, W.A., (2001) "Turbojet and Turbofan Engine Performance Increases Through Turbine Burners," *J. Propulsion and Power*, **17**(3), pp. 695-705.
- Magnussen, B.F. and Hjertager, B.H., (1977) "On Mathematical Models of Turbulent Combustion with Special Emphasis on Soot Formation and Combustion," 16th Symposium (International) on Combustion, pp. 719-729, The Combustion Institute, Pittsburgh.
- Peters, N. (2000) "Turbulent Combustion," Cambridge University Press, UK.
- Ryder, R.C. and McDivitt, T., (2000) "Application of the National Combustion Code Towards Industrial Gas Fired Heaters," AIAA-2000-0456.
- Ryder, R.C., Brankovic, A., Bulzan, D.L., Marek, C.J., Parthasarathy, T.A., and Kerans, R.J., (2003) "CFD Definition Study of Interstage Burners in Turbine Engine Transition Ducts," ASME GT2003-38440.
- Turner, M.G., Ryder, R.C., Norris, A., Celestina, M., Moder, J., Liu, N.-S., Adamczyk, J., and Veres, J., (2002) "High Fidelity 3D Turbofan Engine Simulations with Emphasis on Turbomachinery-Combustor Coupling," AIAA-2002-3769.
- Warnatz, J., Maas, U., and Dibble, R.W., (1996) "Combustion," Springer-Verlag, Berlin.

REPORT DOCUMENTATION PAGE

Form Approved
OMB No. 0704-0188

Public reporting burden for this collection of information is estimated to average 1 hour per response, including the time for reviewing instructions, searching existing data sources, gathering and maintaining the data needed, and completing and reviewing the collection of information. Send comments regarding this burden estimate or any other aspect of this collection of information, including suggestions for reducing this burden, to Washington Headquarters Services, Directorate for Information Operations and Reports, 1215 Jefferson Davis Highway, Suite 1204, Arlington, VA 22202-4302, and to the Office of Management and Budget, Paperwork Reduction Project (0704-0188), Washington, DC 20503.

1. AGENCY USE ONLY (<i>Leave blank</i>)	2. REPORT DATE March 2005	3. REPORT TYPE AND DATES COVERED Technical Memorandum	
4. TITLE AND SUBTITLE Modeling of a Sequential Two-Stage Combustor		5. FUNDING NUMBERS Cost Center 2250000013	
6. AUTHOR(S) R.C. Hendricks, N.-S. Liu, J.R. Gallagher, R.C. Ryder, A. Brankovic, and J.A. Hendricks			
7. PERFORMING ORGANIZATION NAME(S) AND ADDRESS(ES) National Aeronautics and Space Administration John H. Glenn Research Center at Lewis Field Cleveland, Ohio 44135-3191		8. PERFORMING ORGANIZATION REPORT NUMBER E-14193	
9. SPONSORING/MONITORING AGENCY NAME(S) AND ADDRESS(ES) National Aeronautics and Space Administration Washington, DC 20546-0001		10. SPONSORING/MONITORING AGENCY REPORT NUMBER NASA TM-2005-212631 ISROMAC10-2004-037	
11. SUPPLEMENTARY NOTES This report contains a supplemental CD with information on the Wedge Assembly Air Solid Model. Portions of this material were presented at the 10th International Symposium on Transport Phenomena and Dynamics of Rotating Machinery sponsored by the Pacific Center of Thermal Fluids Engineering, Honolulu, Hawaii, March 7-11, 2004. R.C. Hendricks, N.-S. Liu, and J.R. Gallagher, NASA Glenn Research Center; R.C. Ryder and A. Brankovic, Flow Parametrics, Bear, Delaware 19701; and J.A. Hendricks, Diligent Design, Toledo, Ohio 43614. Responsible person, R.C. Hendricks, organization code R, 216-977-7507.			
12a. DISTRIBUTION/AVAILABILITY STATEMENT Unclassified - Unlimited Subject Category: 07 Available electronically at http://gltrs.grc.nasa.gov This publication is available from the NASA Center for AeroSpace Information, 301-621-0390.		12b. DISTRIBUTION CODE	
13. ABSTRACT (<i>Maximum 200 words</i>) A sequential two-stage, natural gas fueled power generation combustion system is modeled to examine the fundamental aerodynamic and combustion characteristics of the system. The modeling methodology includes CAD-based geometry definition, and combustion computational fluid dynamics analysis. Graphical analysis is used to examine the complex vortical patterns in each component, identifying sources of pressure loss. The simulations demonstrate the importance of including the rotating high-pressure turbine blades in the computation, as this results in direct computation of combustion within the first turbine stage, and accurate simulation of the flow in the second combustion stage. The direct computation of hot-streaks through the rotating high-pressure turbine stage leads to improved understanding of the aerodynamic relationships between the primary and secondary combustors and the turbomachinery.			
14. SUBJECT TERMS Combustor; Modeling; CFD; Sequential staged combustion; Fluid mechanics			15. NUMBER OF PAGES 23
			16. PRICE CODE
17. SECURITY CLASSIFICATION OF REPORT Unclassified	18. SECURITY CLASSIFICATION OF THIS PAGE Unclassified	19. SECURITY CLASSIFICATION OF ABSTRACT Unclassified	20. LIMITATION OF ABSTRACT

